A Gyrotron-Traveling-Wave Tube Amplifier Experiment With a Ceramic Loaded Interaction Region

Morag Garven, *Member, IEEE*, J. P. Calame, *Member, IEEE*, Bruce G. Danly, *Senior Member, IEEE*, Khanh T. Nguyen, Baruch Levush, *Fellow, IEEE*, F. N. Wood, and Dean E. Pershing

***Abstract*—The design and experimental study of a 35-GHz gyrotron-traveling-wave tube (gyro-TWT) amplifier operating in the circular TE_{01} mode at the fundamental cyclotron harmonic are presented. The interaction circuit in this experiment consisted of a new type of ceramic loading that provided the required loss for stable operation. A saturated peak power of 137 kW was measured at 34.1 GHz, corresponding to a saturated gain of 47.0 dB and an efficiency of 17%, with a −3-dB bandwidth of 1.11 GHz (3.3%). Peak output powers in the range of 102.1 to 148.6 kW with −3-dB bandwidths of 1.26 and 0.94 GHz, respectively, were measured by varying the operating parameters. The gyro-TWT was found to be zero-drive stable at these operating points, demonstrating that ceramic loading is a highly effective means of suppressing spurious oscillations in gyro-TWTs. This type of ceramic loading has the added advantage of being compatible with high average power operation.**

***Index Terms*—Ceramic loading, electron beam, gyro-traveling wave tube (gyro-TWT), millimeter-wave amplifier.**

I. Introduction

GYROTRON amplifiers are being developed for a variety of applications that require high power in the millimeter wavelength range [1], [2]. In particular, high-average power gyrotron-traveling wave tubes (gyro-TWTs) are being developed at the Naval Research Laboratory (NRL), Washington, DC, for radar applications, both in the TE_{01} mode, as presented in this paper, and in the TE_{11} mode, discussed elsewhere [3], [4]. Gyro-TWTs offer broader bandwidth than gyroklystrons but their high-power capability has been somewhat limited in the past due to spurious oscillations. Recently however, high gain and power were demonstrated in a gyro-TWT amplifier operating in the TE_{11} mode by using distributed wall losses to suppress spurious oscillations [5], [6]. In this paper, we present a new method of stabilizing the gyro-TWT that involves controlled loading of both the TE_{01} operating mode and the backward wave oscillations. A high thermal conductivity, lossy ceramic material was used to suppress oscillations with the added advantage of being high-average power compatible [7].

Gyro-TWT research in various frequency ranges has been conducted over the last two decades. Early 35-GHz gyro-TWT research included an experiment at the NRL, which produced 16.6-kW peak power, 20-dB saturated gain, 7.8% efficiency with a 3-dB bandwidth of 1.5% [8]. A later two-stage tapered gyro-TWT experiment, also at NRL, produced 8 kW power, 25 dB saturated gain, 16% efficiency, and an impressive 3-dB bandwidth of 20% [9]. Harmonic gyro-TWTs have been investigated at the University of California, Davis, CA, where a second harmonic gyro-TWT in the Ku-band produced 207 kW output power, 16 dB saturated gain with 12.9% efficiency, and a bandwidth of 2.1% [10]. Third [11] and even sixth [12] harmonic gyro-TWTs have been investigated. Also at the University of California, a gyro-TWT partially loaded with dielectric produced 55 kW peak output power, 27 dB saturated gain, and a −3 dB bandwidth of 11% in the X-band frequency range [13]. Recently, at the National Tsing Hua University (NTHU), Taiwan, an ultrahigh gain gyro-TWT amplifier produced 93 kW peak power, with 70 dB saturated gain, 26.5% efficiency, and a −3 dB bandwidth of 8.6% [5], [6]. This unprecedented gain from a gyro-TWT was achieved by employing distributed wall losses to suppress spurious oscillations. Other gyro-TWT work is being performed at the University of California at 94 GHz [14], at the University of Maryland, College Park, at 32 GHz [15], [16], and a 35 GHz spiral waveguide gyro-TWT has been demonstrated by a collaboration between the University of Strathclyde, Glasgow, U.K., and the Institute of Applied Physics, Nizhny Novgorod, Russia, [17].

The dispersion relation for the TE_{01} gyro-TWT experiment is shown in Fig. 1 where frequency in Gigahertz is plotted versus axial wavenumber (k_z) in cm^{-1} for the TE_{11}, TE_{21}, TE_{01}, and TE_{02} waveguide modes. The fundamental ($s = 1$) and second ($s = 2$) cyclotron harmonic beam-wave resonance lines are also plotted for a beam voltage of 70 kV, beam alpha of 1.00, magnetic field of 12.61 kG, and a waveguide radius of 0.5495 cm. Beam alpha (α) is defined as the ratio of beam transverse and axial velocities ($v_\perp/v_z$). The gyro-TWT interaction occurs at

Manuscript received November 1, 2001; revised March 8, 2002. This work was supported by the Office of Naval Research and by the Naval Research Laboratory.

M. Garven is with the Vacuum Electronics Branch, U.S. Naval Research Laboratory, Washington, DC 20375 USA and also with Omega-P Inc., New Haven, CT 06520 USA (e-mail: garven@nrl.navy.mil).

J. P. Calame, B. G. Danly, and B. Levush are with the Vacuum Electronics Branch, U.S. Naval Research Laboratory, Washington, DC 20375 USA.

K. T. Nguyen is with the Vacuum Electronics Branch, U.S. Naval Research Laboratory, Washington, DC 20375 USA and also with KN Research, Silver Spring, MD 20905 USA.

F. N. Wood is with the Vacuum Electronics Branch, U.S. Naval Research Laboratory, Washington, DC 20375 USA and also with Dyncorp, Rockville, MD 20850 USA.

D. E. Pershing is with the Vacuum Electronics Branch, U.S. Naval Research Laboratory, Washington, DC 20375 USA and also with Mission Research Corporation, Newington, VA 22122 USA.

Digital Object Identifier 10.1109/TPS.2002.801650

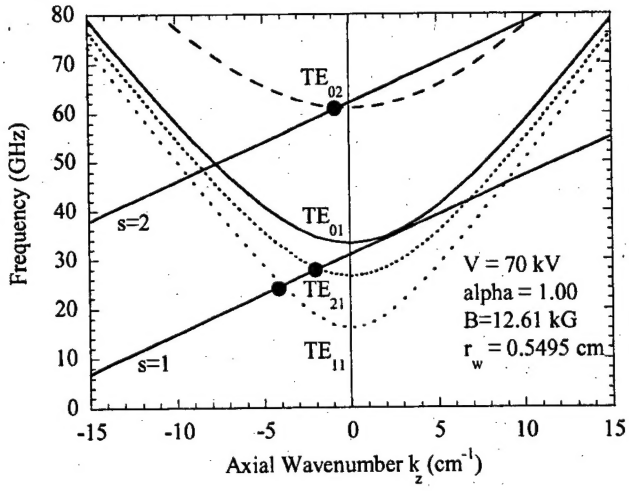

Fig. 1. The dispersion relation for the fundamental TE_{01} gyro-TWT interaction with possible gyro-BWOs shown as solid circles.

the intersection of the fundamental ($s = 1$) beam line and the TE_{01} waveguide mode (solid lines intersection in Fig. 1). Undesirable interactions in the backward wave regime (negative k_z) may cause backward wave oscillations (BWOs) and are shown by the solid circles in Fig. 1. These BWOs were the limiting factor in early gyro-TWT experiments and need to be eliminated to ensure stable operation.

Different types of distributed losses in gyro-TWTs have been investigated including thin lossy coatings [5] and slotted waveguides with lossy material [11]. In our gyro-TWT experiment, we employed a long loaded section of constant radius which consisted of lossy ceramic rings spaced with metal rings to provide controlled loading of the fundamental TE_{01} operating mode. This loading scheme also suppressed spurious backward wave oscillations in the fundamental TE_{11}, TE_{21}, and second harmonic TE_{02} modes. The ceramic elements were made of Ceradyne 80% aluminum nitride (AlN)—20% silicon carbide (SiC) by weight. The nonlinear, highest power portion of the amplification occurred in a short conducting wall section at the end of the interaction region. While this experiment was a low-duty demonstration, the use of high thermal conductivity ceramic should allow for high-average power operation with the addition of ceramic to metal brazing and water cooling.

The remainder of the paper is organized as follows. In Section II, the detailed design, using numerical simulations, and experimental setup of the gyro-TWT are presented. The experimental results and stability studies are reported in Section III. The conclusions and future plans are discussed in Section IV.

II. Experimental Design

A. TE_{01} Gyro-TWT Circuit Design

A schematic diagram of the gyro-TWT experiment is shown in Fig. 2. The gyro-TWT circuit consisted of the input coupler, the loaded interaction section, the unloaded interaction section, and the nonlinear output taper. The detailed design of these components is discussed in this section.

The input coupler was designed using the High-Frequency Structure Simulator (Ansoft's HFSS) to operate in the TE_{01}

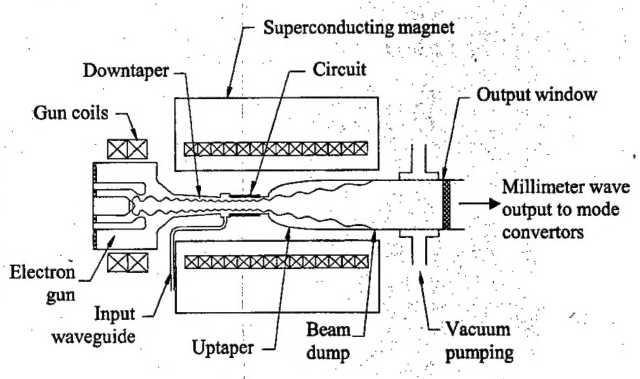

Fig. 2. A schematic drawing of the 35 GHz gyro-TWT experiment.

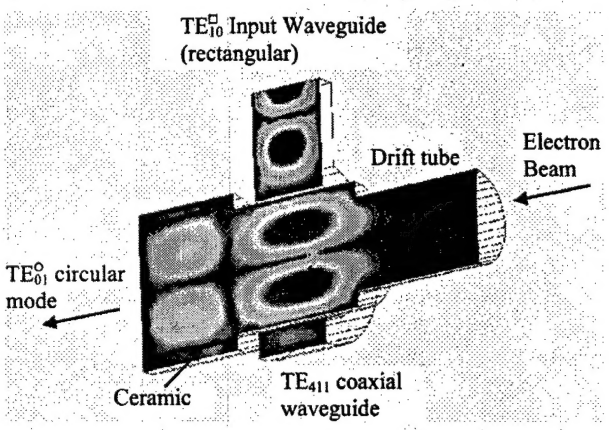

Fig. 3. (a) HFSS simulation of the TE_{01} input coupler design. The field is shown propagating through to the circuit with one ceramic ring modeled. (b) Comparison between the designed (HFSS) and measured transmitted power versus frequency with no ceramic ring included.

mode across the band of 33.3–36 GHz. The input coupler design used a traveling wave version of the rectangular to coaxial chamber to circular beam tunnel geometry used previously in gyroklystron experiments [18] and was similar to that designed by McDermott *et al.* [14]. Fig. 3(a) shows an HFSS simulation of the input coupler, where the electron beam proceeds from the drift tube (below cutoff) to the input coupler and on to the ceramic loaded interaction circuit (one ceramic ring was modeled). The drive signal was injected into a rectangular, Ka-band,

waveguide port which connected to a cylindrical coaxial cavity. The input was the fundamental TE_{10} rectangular mode that coupled via a rectangular aperture to the TE_{411} coaxial cavity mode. Four rectangular apertures spaced 90° in azimuth enabled the TE_{411} mode to couple to the operating TE_{01} cylindrical mode. These four coupling slots were positioned such that the magnetic field of the TE_{411} mode at the slots was aligned to that of the TE_{01} mode in the central coupler.

Cold test measurements of the input coupler with no ceramic loading were performed with good agreement found between theory (HFSS) and measurements, as shown in Fig. 3(b). The transmission measurement resulted in an input coupler loss of $\approx$0.25 dB at 34 GHz and > -2 dB coupling from 33.5 to 35.5 GHz. The input coupler reflected power was measured to be < -5 dB in the operating mode with < -25 dB coupling to the TE_{11} and TE_{21} modes across this band. The total length of the unloaded input coupler was 1.5 cm, which was well below the critical length for start oscillation for all modes as calculated from linear theory [19]. The inner radius of the cylindrical input coupler was the same as the circuit radius (0.5495 cm), hence the TE_{01} mode propagated on to the gyro-TWT interaction region with no step or taper.

The gyro-TWT interaction circuit was designed using the self-consistent, time-dependent, quasi-three-dimensional code MAGY [20]. This code was previously used to design and model gyroklystron amplifiers [21] and was also used to design a TE_{11} gyro-TWT [3]. The lengths of the loaded and unloaded sections were chosen to satisfy stability constraints as well as overall amplifier gain, bandwidth, and efficiency performance based on linear theory calculations [19] and MAGY simulations. The critical oscillation lengths of any spurious modes for an unloaded waveguide of radius 0.5495 cm were calculated and the limiting length was determined to be 4.55 cm for the TE_{02} second harmonic mode. Hence, the copper unloaded section was chosen to be 4 cm in length to ensure stability.

The total length of the interaction region was extended by introducing a loaded region, which allowed for high gain, stable operation. The required loss rate for stability of the TE_{01} operating mode was calculated to be 3.44 dB/cm at 35 GHz [7]. The corresponding loss rates for the BWO modes, TE_{11}, TE_{21}, TE_{02} were 3.04 dB/cm at 25 GHz, 12.5 dB/cm at 28 GHz, and 18.4 dB/cm at 61 GHz, respectively. This loss was included in the MAGY calculations and stability of the TE_{01} mode and the BWO modes was investigated. Simulations indicated that this loss rate was sufficient to suppress all oscillations for beam currents of 8–12 A, beam voltages of 65–75 kV, and beam alphas of 0.9–1.10.

The required cold loss of 3.44 dB/cm at 35 GHz in the TE_{01} operating mode was achieved by using ceramic rings of length 1 cm and an inner radius of 0.5495 cm made of 80% AlN—20% SiC. The complex dielectric permittivity was $\varepsilon^* = \varepsilon' - j\varepsilon'' = 11 - 2.2j$, which was experimentally measured at 35 GHz for 80% AlN—20% SiC at room temperature [22] and the thermal conductivity was $\approx$35 $Wm^{-1}K^{-1}$. The radial thickness of the ceramic was 0.14 cm and was chosen to be where the TE_{02} mode attenuation reaches a minimum that occurs when the field at the dielectric is small. This resulted in the field structure in the vacuum being close to that of the unloaded TE_{01} mode with a similar propagation constant [7]. The total loaded interaction region of 23-cm length and 0.5495-cm radius consisted of 20 ceramic rings alternating with copper rings of 0.15-cm length. The copper rings were incorporated into the design for ease of assembly and to help collect stray electrons that could potentially cause breakdown. Also, including metal rings allows the loading of nonaxisymmetric parasitic modes to be adjusted selectively due to the absence of axial currents in the TE_{0n} modes [7].

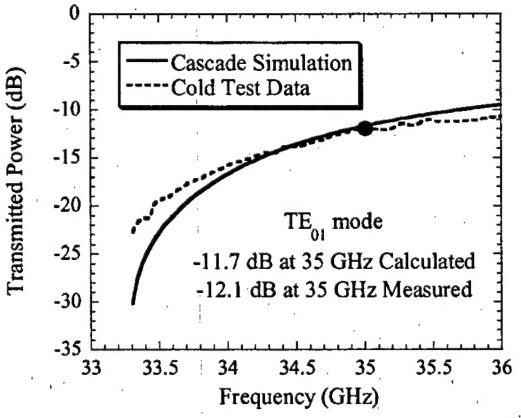

Fig. 4. Measured cold test results for three circuit ceramics and comparison with theory for the TE_{01} operating mode.

The cold test, transmission properties of three circuit ceramics plus copper rings (total length 3.45 cm) were measured for the TE_{01} operating mode. The cold loss was calculated by using a known value of the loss tangent ($\tan\delta = 0.20$) for 80% AlN—20% SiC at 35 GHz [22]. Fig. 4 shows the measured cold test results for three circuit ceramics compared with calculations performed using a version of CASCADE [23] which was modified to include lossy, dielectric material. The cold loss for the TE_{01} mode was measured to be 3.51 dB/cm at 35 GHz, which agreed well with both the CASCADE value of 3.39 dB/cm and the theoretically calculated value of 3.44 dB/cm at 35 GHz [7]. Similar agreement was obtained for a measurement of the TE_{11} mode.

A schematic of the circuit geometry in Fig. 5(a) shows the input coupler, 23-cm loaded section and 4-cm unloaded section all with the same continuous wall radius of 0.5495 cm. The magnetic field profile and calculated spatial power (MAGY) profile at 35 GHz for a 65-kV 10-A alpha = 0.90 electron beam are also shown. The power profile clearly illustrates the low power, linear stage of amplification in the loaded interaction region and the high-power nonlinear stage in the short unloaded region. In this simulation, the magnetic field was set at 98% of the grazing field in the interaction section of the circuit. The nonlinear uptaper was designed to minimize reflection of the operating mode and to ensure minimal mode conversion. Return loss from the uptaper was cold tested and measured to be below -20 dB across the band, as necessary to avoid any spurious oscillations or reflections. The start oscillation currents for the TE_{01} operating mode and for the BWOs, including the problematic second harmonic TE_{02} mode, were calculated and found to be above the planned operating current range of 8–11 A.

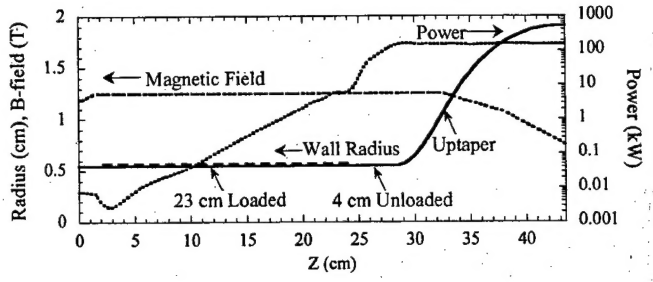

(a)

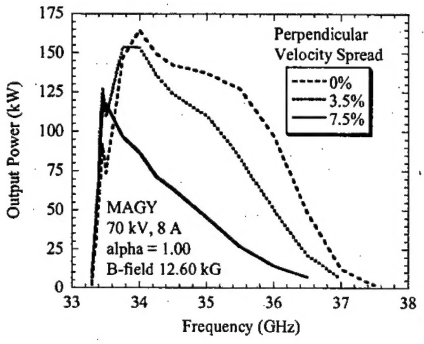

(b)

Fig. 5. MAGY simulations of the gyro-TWT experiment. (a) Geometry, magnetic field, and calculated output power. (b) Simulations demonstrating the effect of perpendicular velocity spread on output power and bandwidth.

The performance of the gyro-TWT was calculated using MAGY and the effect of velocity spread on bandwidth is clearly illustrated in Fig. 5(b). For the ideal case of 0% perpendicular velocity spread, a peak power of 165 kW was calculated with a saturated gain of 43 dB, an efficiency of 30%, and a -3 dB bandwidth of 2.7 GHz ($\approx$8%). In these simulations, increasing the velocity spread resulted in reduced output power and bandwidth. For a perpendicular velocity spread of 7.5%, a reduced peak power of 118 kW was calculated with a -3 dB bandwidth of 1.25 GHz ($\approx$4%). The electron gun used in this experiment had a high perpendicular velocity spread, in the region of 8%–10%, since it was previously designed for higher beam voltage (80 kV) and alpha operation (1.4) for a different application. This high value of perpendicular velocity spread was undesirable for optimum bandwidth operation of the gyro-TWT, as shown from Fig. 5(b), but was deemed acceptable for an initial gyro-TWT demonstration of the ceramic loading scheme. MAGY simulations indicated that reasonable output power, gain, and bandwidth were still achievable with this high value of velocity spread for a proof-of-principle experiment. Clearly, the future substitution of a higher quality electron gun would significantly improve the performance of this gyro-TWT in terms of peak power and bandwidth.

B. Experimental Setup

The gyro-TWT experimental setup was similar to that of previous 35 GHz gyroklystron experiments [24], [25] and is shown schematically in Fig. 2. The experiment consisted of the electron gun, magnetic field, input source, input coupler, gyro-TWT circuit, beam collector, output windows, and RF measurement diagnostics. The detailed input coupler and gyro-TWT circuit

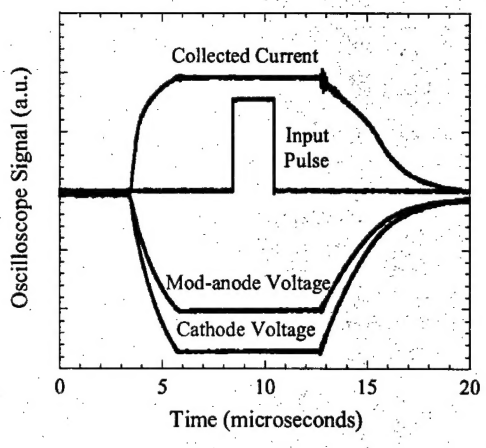

Fig. 6. Typical measured waveforms of the input pulse, cathode voltage, modulating anode voltage, and collected beam current from the gyro-TWT.

design were described in the previous section. The remaining components are described in this section.

The electron beam was produced from a thermionic, double anode, magnetron injection gun (CPI model VUW-8035) with beam voltages of 70–72 kV and beam currents of 8–11 A for this experiment. Typical voltage, current, and input pulse waveforms are shown in Fig. 6. The input pulse was positioned in the center of the flat region of the voltage and current waveforms for these experiments.

The electron beam was adiabatically compressed from the MIG to the circuit region by a solenoidal magnetic field. The uniform interaction field of typically 12.60 kG was generated by a variable 14-coil superconducting magnet with the gyro-TWT circuit positioned in this flat field region. Two conventional water cooled gun coils provided control of cathode magnetic field and, hence, beam alpha during the experiment. A capacitive probe was used to measure alpha and was calibrated using a numerical finite difference method [25].

After the unloaded high-gain section of the gyro-TWT, the spent electron beam and the high power RF entered a nonlinear uptaper followed by a copper, water-cooled collector or beam dump (Fig. 2). Gradual deposition of the electron beam was achieved by decreasing the magnetic field profile through the nonlinear uptaper and beam collector regions. The collector also functioned as the output waveguide between the RF circuit and the output windows.

A double disk output window assembly was designed to provide broad bandwidth performance. Two BeO disks of half-wavelength thickness (0.17 cm) were spaced 0.26 cm apart to provide less than -20 dB reflection over 2.5-GHz bandwidth centered at 34.5 GHz. The first BeO disk provided the vacuum seal to the experiment and the second disk was positioned in air. The experiment operated under a high vacuum of $\sim 1 \times 10^{-8}$ torr.

The output power was measured using an anechoic chamber [26] with a pickup antenna positioned at the angle of the maximum of the TE_{01} mode radiation pattern (11.5°). This antenna could be swept in polar angle relative to the central axis of the experiment to measure radiation patterns. Cold tests with the input source and power meters were used to calibrate this chamber. The peak output power pulse was observed and

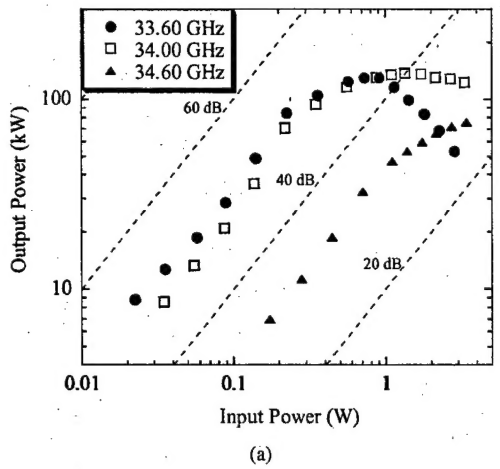

(a)

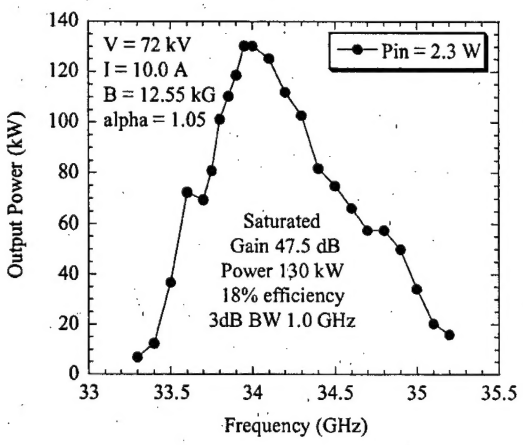

(b)

Fig. 7. (a) Measured peak output power versus input power for three drive frequencies of 33.60, 34.00, and 34.60 GHz. (b) Measured output power versus frequency for a constant input power of 2.3 W.

measured during these experiments using a calibrated HP peak power analyzer setup in conjunction with the cold test calibration, and the estimated systematic accuracy was ±7%.

The input source was a 26.5–40 GHz 10-W continuous wave traveling wave tube (Hughes model 8010H12). This TWT was pulsed to produce 2-μs input signals with a repetition rate of 2 Hz for these experiments. The TWT output power was varied by using a rotary attenuator. A bi-directional coupler allowed the measurement of the input and reflected powers using calibrated attenuator, sensor, and peak power analyzer assemblies. The input frequency was determined by the HP sweeper used to drive the Hughes TWT.

III. Experimental Results and Discussion

A. Peak Power and Bandwidth Studies

Experiments were performed to study the operating characteristics of the gyro-TWT. An initial study of the optimum operation of the gyro-TWT amplifier in terms of peak output power and bandwidth was undertaken while also ensuring that the device was zero drive stable. For the purpose of this experimental discussion, bandwidth refers to the −3 dB bandwidth. Fig. 7(a) shows drive curves measured at three different frequencies for a beam voltage of 72 kV, beam current of 10 A, magnetic field

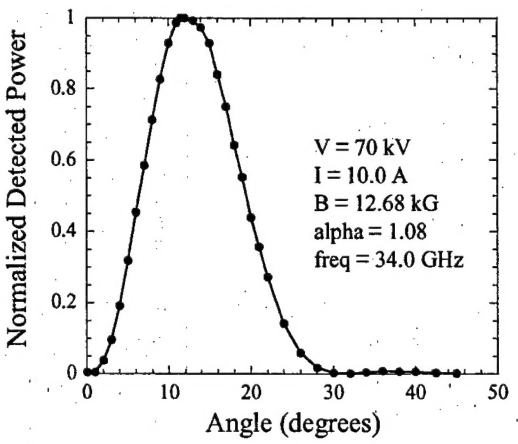

Fig. 8. TE_{01} output mode pattern measured using the anechoic chamber.

of 12.55 kG, and a beam alpha of 1.05, all held constant. From these results, a drive power of 2.3 W was chosen to maximize bandwidth and the frequency response was measured for these constant beam parameters. A peak power of 130 kW was measured at 34.0 GHz corresponding to a saturated gain of 47.5 dB and an efficiency of 18%, Fig. 7(b). The bandwidth for this case was 1.0 GHz (3%). Further studies involved varying the magnetic field, current, voltage, and alpha around these values.

Fig. 8 shows the TE_{01} mode pattern scan measured using the anechoic chamber. The angle of the pickup antenna was varied from 0° to 45° while the output power was measured. The detected power has been normalized to its maximum value and the radiation pattern in Fig. 8 was measured at a nominal operating point that produced a saturated power of 130 kW, gain of 52 dB, and an efficiency of 19% for a frequency of 34.0 GHz. This mode pattern scan was measured with a beam voltage of 70 kV, 10-A beam current, alpha of 1.08, and a magnetic field of 12.68 kG and was consistent with a TE_{01} radiation mode pattern.

The dependence of peak output power on input drive power for a range of frequencies was investigated. Fig. 9 shows measurements taken with a magnetic field setting of 12.56 kG, a beam voltage of 70 kV, a beam current of 10 A, and a beam alpha of 1.08. With these values held constant, the drive curves were measured for four different frequencies as shown in Fig. 9(a). The required input power to saturate ranged from 0.07 W for a drive frequency of 33.50 GHz to 0.85 W at 34.00 GHz while 2.5 W was not enough power to saturate at 34.30 GHz. The maximum achievable input drive power was ≈2.5 W due to input power line and input coupler losses.

The frequency responses for a range of input powers were measured, at the previous settings, as shown in Fig. 9(b). With a constant input power of 0.25 W, a peak output power of 120 kW was measured at a frequency of 33.95 GHz and the bandwidth was 0.70 GHz. Increasing the drive power resulted in an increase in peak output power and bandwidth. For a 0.80-W drive, a peak output power of 133 kW was measured at 33.95 GHz with 0.77-GHz bandwidth. Increasing the drive power further resulted in broader bandwidth with slightly reduced output power. For example, with 1.70-W input power, a peak output power of 121 kW was measured at 34.10 GHz with an increased bandwidth of

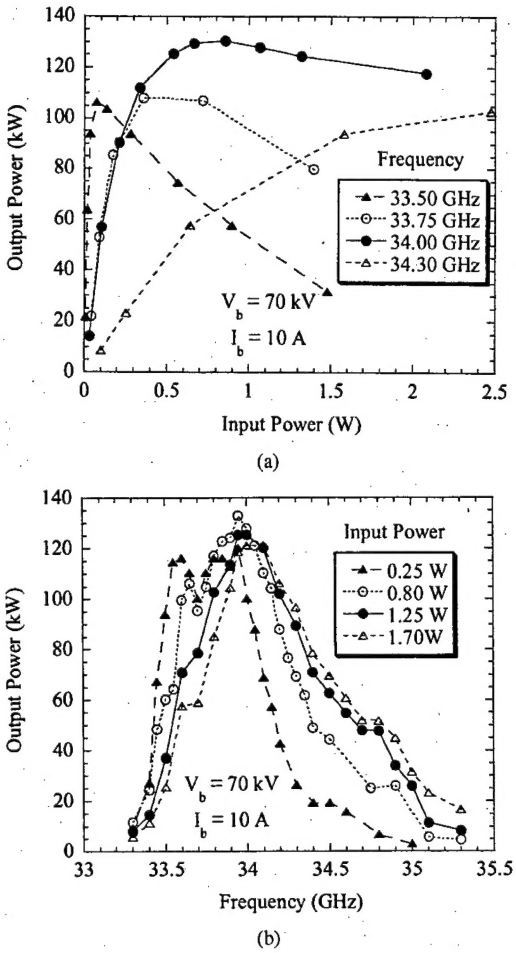

Fig. 9. (a) Measured output power versus input power for a range of frequencies. (b) Peak output power versus frequency showing the power and bandwidth dependence on input power.

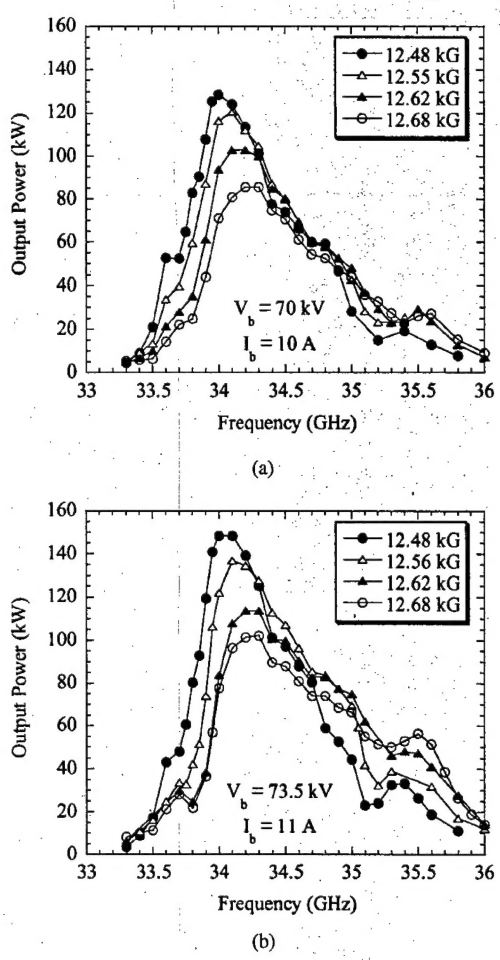

Fig. 10. Measured frequency responses with increasing magnetic field for (a) beam voltage of 70 kV, beam current of 10 A, and (b) beam voltage of 73.5 kV, beam current of 11 A.

0.90 GHz. The increase in peak frequency with drive power was a result of the low-frequency end of the band being over-saturated. The gyro-TWT amplifier demonstrated a tradeoff in terms of peak output power versus bandwidth, which was obtained by varying the input drive power for constant magnetic field, voltage, current, and beam alpha.

The behavior of the gyro-TWT interaction with varying magnetic field was also investigated. In Fig. 10(a), for a beam voltage of 70 kV, current of 10 A, alpha of 1.08, and drive power of 2.5 W all held constant, the magnetic field was increased from 12.48 to 12.68 kG. Increasing the magnetic field had the effect of increasing the bandwidth at the expense of peak output power. There was also a corresponding increase in peak frequency with increased magnetic field. For example, with the magnetic field setting of 12.48 kG, a peak power of 128.6 kW was measured at 34.0 GHz with a bandwidth of 0.88 GHz. At the highest magnetic field of 12.68 kG, the bandwidth increased to 1.10 GHz and the peak power was 85.5 kW at 34.3 GHz.

A similar study was performed for higher beam current and voltage of 11 A and 73.5 kV, respectively. As shown in Fig. 10(b), higher beam power resulted in higher output power and broader bandwidth. With a magnetic field setting of 12.48 kG, a peak power of 148.6 kW was measured at 34.0 GHz with a bandwidth of 0.94 GHz. As the magnetic field was increased to 12.55 kG, the power reduced to 136.9 kW at 34.1 GHz while the bandwidth increased to 1.11 GHz (3.33%). At the highest field of 12.68 kG, the bandwidth increased to 1.26 GHz with a reduced output power of 102.1 kW at 34.3 GHz.

B. Stability of the Gyro-TWT

The stability of the gyro-TWT was of great interest due to the new ceramic loading scheme. Stability measurements were performed with no input signal while the electron beam was propagating. The TE_{01} operating mode was observed using the output power peak analyzer setup described in Section II-B. A second, higher frequency pickup waveguide (60–70 GHz) was positioned at an angle of 3.4° to detect the second harmonic TE_{02} mode. This detector was not calibrated due to the lack of a suitable source, however the response gave a crude indication of the presence of the second harmonic TE_{02} mode expected to be at ≈61 GHz.

It should be noted that the gyro-TWT was zero-drive stable for all plots discussed in the previous results section. However, if the beam alpha was increased at the various magnetic field settings with the drive off, then an instability was eventually

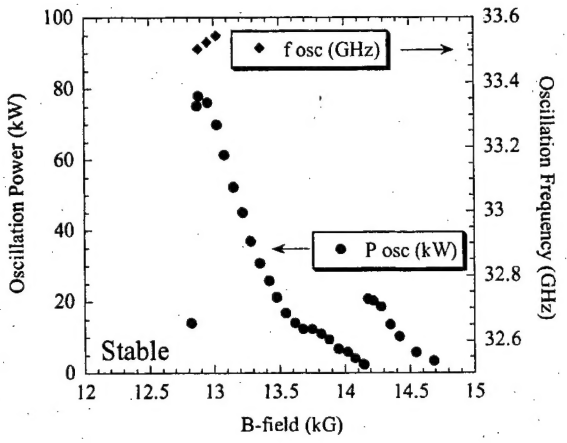

Fig. 11. Measured power and frequency of spurious oscillations versus magnetic field for zero-drive power. The optimum operating regime for the TE_{01} gyro-TWT amplifier was in the stable region.

observed and identified as a self-oscillation of the TE_{01} operating mode. As alpha was increased further, the TE_{02} second harmonic instability was also detected and appeared to suppress the TE_{01} mode as alpha was increased even further.

Localized reflective oscillations have been calculated and measured for a TE_{11} mode gyro-TWT by Chu *et al.* [5]. These oscillations occur in the unloaded section of the gyro-TWT due to reflections at the ceramic to metal and output taper transitions. These localized oscillations were observed in this TE_{01} gyro-TWT experiment by increasing the magnetic field above the optimum region for amplification. The measured oscillation power and frequency as a function of interaction magnetic field are shown in Fig. 11. With the drive power off, the magnetic field was increased while the TE_{01} mode and TE_{02} mode detectors were monitored. The TE_{011} gyromonotron-like oscillation was observed to have a very sharp rise in power $\approx$80 kW in the magnetic field region of 12.88 kG with a frequency of $\approx$33.5 GHz recorded. As the magnetic field was increased beyond 13 kG, no reliable frequency was recorded due to mode jumping between the TE_{01} axial modes. These measurements were consistent with previously published gyro-TWT theory and results [5], and demonstrated the existence of localized reflective oscillations in this experiment at high magnetic fields.

IV. Conclusion

A 35 GHz gyro-TWT with a ceramic loaded interaction region was designed and operated in the circular TE_{01} mode at the fundamental harmonic. By varying system parameters, this gyro-TWT achieved peak output powers in the range of 102.1–148.6 kW with bandwidths of 1.26 and 0.94 GHz, respectively. The stability of this device was excellent, demonstrating that ceramic loading is a highly effective means of suppressing spurious oscillations in gyro-TWTs. This proof-of-principle device operated with low duty cycle, but the design used a high thermal conductivity, ceramic loaded section that requires only ceramic to metal brazing and water cooling to be high-average power compatible. The peak ohmic power dissipated in the highest gain section of the loading (the final ceramic element of 1 cm length) was calculated to be $\approx$6.5 kW for a peak output power of $\approx$150 kW. Assuming a 10% duty factor, this corresponds to an average power loss of $\approx$190 W/cm^2 in the final ceramic, which is comparable to the power loading of ceramics in a high-average power gyroklystron [21]. Further investigation of the high-average power compatibility of the loading scheme will be undertaken in the future.

This gyro-TWT was designed using MAGY. Further studies and comparisons will be performed to fully understand and model the ceramic loading scheme using a new version of MAGY that includes lossy materials [27]. The bandwidth of this gyro-TWT was limited by the performance of the electron gun, which had a perpendicular velocity spread of $\approx$8%–10%. Simulations indicated that by reducing the velocity spread, the bandwidth could be more than doubled. The components of the TE_{01} gyro-TWT were designed to be compatible with a lower velocity spread electron gun and for optimum bandwidth operation. The input coupler and double disk output windows were both measured to have a -3 dB bandwidth of 2.5 GHz. Hence, this experiment could be upgraded to a higher average power, broader bandwidth gyro-TWT in the future.

Acknowledgment

The authors would like to thank Dr. J. L. Hirshfield and Dr. S. J. Cooke for many useful discussions. They also acknowledge excellent technical support from R. Myers, F. Robertson, B. Sobocinski, G. Longrie, and D. Lobas.

References

[1] K. L. Felch, B. G. Danly, H. R. Jory, K. E. Kreischer, W. Lawson, B. Levush, and R. J. Temkin, "Characteristics and applications of fast-wave gyrodevices," *Proc. IEEE*, vol. 87, pp. 752–781, May 1999.

[2] V. L. Granatstein, B. Levush, B. G. Danly, and R. K. Parker, "A quarter century of gyrotron research and development," *IEEE Trans. Plasma Sci.*, vol. 25, pp. 1322–1335, Dec. 1997.

[3] K. T. Nguyen, J. P. Calame, D. E. Pershing, B. G. Danly, M. Garven, B. Levush, and T. M. Antonsen, "Design of a *Ka*-band gyro-TWT for radar applications," *IEEE Trans. Plasma Sci.*, vol. 48, pp. 108–115, Feb. 2001.

[4] D. E. Pershing, J. P. Calame, K. T. Nguyen, B. G. Danly, and B. Levush, "A distributed loss technique for high average power gyro-TWTs," in *Proc. 2nd Int. Vacuum Electronics Conf.*, Noordwijk, The Netherlands, Apr. 2001, pp. 145–146.

[5] K. R. Chu, H. Y. Chen, C. L. Hung, T. H. Chang, L. R. Barnett, S. H. Chen, T. T. Yang, and D. J. Dialetis, "Theory and experiment of ultra-high-gain gyrotron traveling wave amplifier," *IEEE Trans. Plasma Sci.*, vol. 27, pp. 391–404, Apr. 1999.

[6] K. R. Chu, H. Y. Chen, C. L. Hung, T. H. Chang, L. R. Barnett, S. H. Chen, and T. T. Yang, "Ultrahigh gain gyrotron traveling wave amplifier," *Phys. Rev. Lett.*, vol. 81, no. 21, pp. 4760–4763, Nov. 1998.

[7] J. P. Calame, M. Garven, B. G. Danly, B. Levush, and K. T. Nguyen, "Gyrotron-traveling-wave-tube circuits based on lossy ceramics," *IEEE Trans. Electron Devices*, vol. 49, pp. 1469–1477, Aug. 2002.

[8] L. R. Barnett, K. R. Chu, J. M. Baird, V. L. Granatstein, and A. T. Drobot, "Gain, saturation, and bandwidth measurements of the NRL gyrotron travelling wave amplifier," in *Proc. Tech. Dig. Int. Electron Devices Meeting*. New York, 1979, pp. 164–167.

[9] G. S. Park, J. J. Choi, S. Y. Park, C. M. Armstrong, A. K. Ganguly, R. H. Kyser, and R. K. Parker, "Gain broadening of two-stage tapered traveling wave tube amplifier," *Phys. Rev. Lett.*, vol. 74, no. 12, pp. 2399–2402, Mar. 1995.

[10] Q. S. Wang, D. B. McDermott, and N. C. Luhmann, Jr., "Operation of a stable 200 kW second harmonic gyro-TWT amplifier," *IEEE Trans. Plasma Sci.*, vol. 24, pp. 700–706, June 1996.

[11] C. K. Chong, D. B. McDermott, and N. C. Luhmann, Jr., "Slotted third-harmonic gyro-TWT amplifier experiment," *IEEE Trans. Plasma Sci.*, vol. 24, pp. 727–734, June 1996.

[12] D. S. Furuno, D. B. McDermott, C. S. Kou, N. C. Luhmann, Jr., and P. Vitello, "Theoretical and experimental investigation of a high-harmonic gyro-traveling-wave tube amplifier," *Phys. Rev. Lett.*, vol. 62, no. 11, pp. 1314–1317, Mar. 1989.

[13] K. C. Leou, D. B. McDermott, C. K. Chong, and N. C. Luhmann, Jr., "Experimental investigation of a broadband dielectric-loaded gyro-TWT amplifier," *IEEE Trans. Electron Devices*, vol. 43, pp. 1016–1020, June 1996.

[14] D. B. McDermott, H. Song, Y. Hirata, A. T. Lin, T. H. Chang, K. R. Chu, and N. C. Luhmann, Jr., "140 kW, 94 GHz heavily loaded TE_{01} gyro-TWT," in *Proc. 2nd Int. Vacuum Electronics Conf.*, Noordwijk, The Netherlands, Apr. 2001, pp. 143–144.

[15] H. Guo, S. H. Chen, V. L. Granatstein, J. Rodgers, G. Nusinovich, M. Walter, B. Levush, and W. J. Chen, "Operation of a highly overmoded, harmonic-multiplying, wideband gyrotron amplifier," *Phys. Rev. Lett.*, vol. 79, no. 3, pp. 515–518, July 1997.

[16] G. S. Nusinovich, J. Rodgers, W. Chen, and V. L. Granatstein, "Phase stability in gyro-traveling-wave-tubes," *IEEE Trans. Electron Devices*, vol. 48, pp. 1460–1468, July 2001.

[17] V. L. Bratman, A. W. Cross, G. G. Denisov, W. He, A. D. R. Phelps, K. Ronald, S. V. Samsonov, C. G. Whyte, and A. R. Young, "High-gain wide-band gyrotron traveling wave amplifier with a helically corrugated waveguide," *Phys. Rev. Lett.*, vol. 84, no. 12, pp. 2746–2749, Mar. 2000.

[18] J. J. Choi, A. H. McCurdy, F. N. Wood, R. H. Kyser, J. P. Calame, K. T. Nguyen, B. G. Danly, T. M. Antonsen, B. Levush, and R. K. Parker, "Experimental investigation of a high power, two-cavity, 35 GHz gyroklystron amplifier," *IEEE Trans. Plasma Sci.*, vol. 26, pp. 416–425, June 1998.

[19] C. S. Kou, Q. S. Wang, D. B. McDermott, A. T. Lin, K. R. Chu, and N. C. Luhmann, Jr., "High power harmonic gyro-TWTs—Part I: Linear theory and oscillation study," *IEEE Trans. Plasma Sci.*, vol. 20, pp. 155–169, June 1992.

[20] M. Botton, T. M. Antonsen, B. Levush, K. T. Nguyen, and A. N. Vlasov, "MAGY: A time-dependent code for simulation of slow and fast microwave devices," *IEEE Trans. Plasma Sci.*, vol. 26, pp. 882–892, June 1998.

[21] K. T. Nguyen, B. Levush, T. M. Antonsen Jr., M. Botton, M. Blank, J. P. Calame, and B. G. Danly, "Modeling of gyroklystrons with MAGY," *IEEE Trans. Plasma Sci.*, vol. 28, pp. 867–886, June 2000.

[22] J. P. Calame, D. K. Abe, B. Levush, and B. G. Danly, "Variable temperature measurements of the complex dielectric permittivity of lossy AlN-SiC composites from 26.5–40 GHz," *J. Appl. Phys.*, vol. 89, no. 10, pp. 5618–5621, May 2001.

[23] J. M. Neilson, P. E. Latham, M. Kaplan, and W. G. Lawson, "Determination of resonant frequencies in complex cavities using the scattering matrix formulation," *IEEE Trans. Microwave Theory Tech.*, vol. 37, pp. 1165–1170, Aug. 1989.

[24] M. Garven, J. P. Calame, K. T. Nguyen, B. G. Danly, B. Levush, and F. N. Wood, "Experimental studies of a four-cavity, 35 GHz gyroklystron amplifier," *IEEE Trans. Plasma Sci.*, vol. 28, pp. 672–680, June 2000.

[25] J. P. Calame, M. Garven, J. J. Choi, K. Nguyen, F. Wood, M. Blank, B. G. Danly, and B. Levush, "Experimental studies of bandwidth and power production in a three-cavity, 35 GHz gyroklystron amplifier," *Phys. Plasmas*, vol. 6, no. 1, pp. 285–297, Jan. 1999.

[26] K. T. Nguyen, J. P. Calame, B. G. Danly, B. Levush, M. Garven, and T. Antonsen, Jr., "Higher order mode excitation in gyro-amplifiers," *Phys. Plasmas*, vol. 8, no. 5, pp. 2488–2494, May 2001.

[27] A. N. Vlasov and T. M. Antonsen, Jr., "Numerical solution of fields in lossy structures using MAGY," *IEEE Trans. Electron Devices*, vol. 48, pp. 45–55, Jan. 2001.

Morag Garven (M'95) received the B.Sc. (with honors) and Ph.D. degrees in physics from the University of Strathclyde, Glasgow, U.K., in 1989 and 1994, respectively. The title of her Ph.D. dissertation was "Novel Gyrotron Experiments Employing a Field Emission Array Cathode," and this work involved an industrial sponsorship with GEC-Marconi Ltd., U.K.

She joined the Vacuum Electronics Branch, Naval Research Laboratory, Washington, DC, in 1995 as an On-Site Contractor with the University of Maryland, College Park. During this time, she participated in the design of a twystrode using a field-emission array cathode. She also investigated gyroklystrons for radar applications. Since 2000, she has been with the Vacuum Electronics Branch as an On-Site Contractor with Omega-P Inc., New Haven, CT. She has been responsible for the design and experimental demonstration of a gyro-TWT amplifier using a novel type of dielectric loading to ensure stability. Her current research interests include experimental high-power microwave devices, including gyroklystrons and gyro-TWTs, and novel sources of microwave radiation.

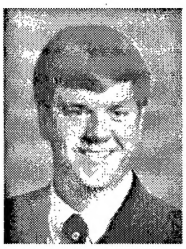

J. P. Calame (M'96) received the B.S., M.S., and Ph.D. degrees in electrical engineering from the University of Maryland, College Park, in 1985, 1986, and 1991, respectively.

From 1980 to 1985, he performed part-time research on the electrical behavior of ionic crystals and ion-conducting polymers at the U.S. Naval Academy Physics Department. His graduate research from 1985 to 1991 involved the development of high peak power gyroklystrons. From 1991 to 1992, he worked with microfabricated field emission electron sources and devices at the Naval Research Laboratory (NRL), Washington, DC. From 1992 to 1997, he studied high power microwave amplifiers, the microwave processing of materials and the dielectric properties of ceramics at the Institute for Plasma Research, University of Maryland, College Park. Presently, he is with the NRL, where he is developing high-average power, wideband millimeter wave amplifiers for radar applications. He is also studying the dielectric and thermal properties of composite ceramic materials and he is investigating intrinsic electronic noise in millimeter wave systems.

Dr. Calame received the 1991 American Physical Society award for Outstanding Doctoral Thesis Research in Beam Physics.

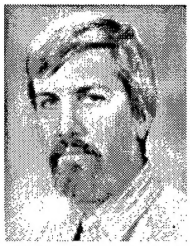

Bruce G. Danly (M'87–SM'01) received the B.A. degree in physics from Haverford College, Haverford, PA, and the Ph.D. degree in physics from the Massachusetts Institute of Technology (MIT), Cambridge, in 1978 and 1983, respectively.

He was on the research staff at the MIT Plasma Fusion Center, first as a Research Scientist from 1983 to 1992 and then as Principal Scientist from 1992 to 1995. While at MIT, he participated in research on gyrotrons, free-electron lasers and relativistic klystrons for use in plasma heating and high-gradient RF linear accelerators. In 1995, he joined the Naval Research Laboratory (NRL), Washington, DC, as Head of the High Power Devices Section, Vacuum Electronics Branch. He is responsible for experimental research and development on high power microwave, millimeter-wave and infrared sources, including gyroklystron, gyro-TWTs, free-electron lasers, TWTs and klystrons. He is also the Program Point of Contact for the High Performance Millimeter Wave Devices Program, administered by the NRL Vacuum Electronics Branch for the Office of Naval Research.

Dr. Danly is a member of the American Physical Society.

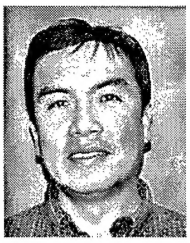

Khanh T. Nguyen received the B.S. degree in physics and mathematics, the M.S. degree in mathematics, and the M.S. and the Ph.D. degrees in nuclear science, all from the University of Michigan, Ann Arbor, in 1978, 1979, 1980, and 1983, respectively. His Ph.D. research topic was a stability study of the ELMO bumpy torus fusion device.

After receiving the Ph.D. degree, he joined the Department of Research and Technology, Naval Surface Warfare Center, White Oak, MD, where he was the Lead Theorist for the charged particle beam propagation experimental program. In 1989, he joined Mission Research Corporation (MRC), Washington DC, as a Senior Scientist, and later became the Leader of the Electromagnetic Application Group. At MRC, his research efforts were in the areas of charged particle beam propagation, vacuum electronics, compact accelerator development, X-ray and γ-ray simulators, and high-power microwave sources development. Since 1994, when he initiated KN Research, Silver Spring, MD, he has been an on-site Contractor with the Vacuum Electronics Branch, Naval Research Laboratory, Washington, DC. His current research interests include the design and modeling of vacuum electronic devices.

Baruch Levush (M'88–SM'90–F'01) received the M.Sc degree in physics from Latvian University, Riga, Latvia, and the Ph.D. degree in Physics from Tel-Aviv University, Israel. In 1985, he joined the Institute for Plasma Research at the University of Maryland, where his research focused on the physics of coherent radiation sources and the design of high-power microwave sources, such as gyrotrons, traveling-wave tubes, backward-wave oscillators and free-electron lasers. In 1995, he joined Naval Research Laboratory, Washington, DC, as the Head of the Theory and Design Section of the Vacuum Electronics Branch, Electronics and Technology Division. He is actively involved in developing theoretical models and computational tools for analyzing the operation of vacuum electron devices and in inventing new concepts for high-power, high-frequency coherent radiation sources. He is responsible for developing a suite of new design codes for vacuum electron devices under the auspices of the Office of Naval Research Modeling and Simulation project. He is the co-author of over 130 journal articles.

Dr. Levush was the recipient of the 1999 Robert L. Woods Award for his role in the successful development of a 10-kW average power, W-band gyroklystron.

F. N. Wood received the B.S. degree in mechanical engineering from George Washington University, Washington, DC, in 1983.

He has been involved in the design of high-power microwave tubes since 1983. He is a Senior Microwave Tube Design Engineer in the Vacuum Electronics Branch, Electronics Science and Technology Division, Naval Research Laboratory (NRL), where he is designing high-power, broad band gyroklystrons and gyro-TWTs as a contractor from Dyncorp (formerly B-K Systems), Rockville, MD. Previously, he was with with the Universities Research Associates, Dallas, TX, where he worked on the design and fabrication of a proton accelerator for the Superconducting SuperCollider.

Dean E. Pershing received the B.S. and Ph.D. degrees in physics from North Carolina State University, Raleigh, in 1971 and 1980, respectively.

In 1980, he continued research on the generation and propagation of intense electron and ion beams as a National Research Council/Naval Research Laboratory (NRL) Postdoctoral Research Associate while participating in the NRL Ion Ring Program. From 1981 to 1983, he participated in the design of the Modified Betatron Accelerator at the NRL, while he was a staff member of JAYCOR, Alexandria, VA. Since joining Mission Research Corporation, Newington, VA, in 1983, his research has concentrated on the design and testing of high-power microwave amplifiers, including ubitron/FELs and, most recently, gyroklystrons and gyro-TWTs.